

1

2 **Predicting Optimal Patient-Specific Postoperative Facial Landmarks for**

3 **Patients with Craniomaxillofacial Deformities**

4

5 Jungwook Lee<sup>1,\*</sup>, Daeseung Kim<sup>2,\*,\*\*</sup>, Xuanang Xu<sup>1</sup>, Tianshu Kuang<sup>2</sup>, Jaime Gateno<sup>2,3</sup>, Pingkun Yan<sup>1,\*\*</sup>

6

7

8 1. Department of Biomedical Engineering and Center for Biotechnology and Interdisciplinary Studies,

9 Rensselaer Polytechnic Institute, Troy, NY 12180, USA

10 2. Department of Oral and Maxillofacial Surgery, Houston Methodist Research Institute,

11 Houston, TX, 77030, USA

12 3. Department of Surgery (Oral and Maxillofacial Surgery), Weill Medical College,

13 Cornell University, New York, NY, 10021, USA

14

15 \* Equally contributed first authors

16 \*\* Co-corresponding authors

17

18

19 **Corresponding authors:**

20 Daeseung Kim, PhD

21 Department of Oral and Maxillofacial Surgery

22 6560 Fannin Street, Suite 1280

23 Houston Methodist Hospital

24 Houston, TX 77030

25 Email: [dkim@houstonmethodist.org](mailto:dkim@houstonmethodist.org)

26 Telephone: (713) 441-8938

27

28 Pingkun Yan, PhD

29 Department of Biomedical Engineering and Center for Biotechnology and Interdisciplinary Studies

30 4231 Biotechnology and Interdisciplinary Studies Building, 110 8th Street

31 Rensselaer Polytechnic Institute

32 Troy NY 12180

33 Email: yanp2@rpi.edu

34 Telephone: (518) 276-4476

35 **1 Abstract**

36 Orthognathic surgery traditionally focuses on correcting skeletal abnormalities and malocclusion, with the  
37 expectation that an optimal facial appearance will naturally follow. However, this skeletal-driven approach can  
38 lead to undesirable facial aesthetics and residual asymmetry. To address these issues, a soft-tissue-driven  
39 planning method has been proposed. This innovative method bases bone movement estimates on the targeted  
40 ideal facial appearance, thus increasing the surgical plan's accuracy and effectiveness. This study explores the  
41 initial phase of implementing a soft-tissue-driven approach, simulating the patient's optimal facial look by  
42 repositioning deformed facial landmarks to an ideal state. The algorithm incorporates symmetrization and  
43 weighted optimization strategies, aligning projected optimal landmarks with standard cephalometric values for  
44 both facial symmetry and form, which are integral to facial aesthetics in orthognathic surgery. It also includes  
45 regularization to preserve the patient's original facial characteristics. Validated using retrospective analysis of  
46 data from both preoperative patients and normal subjects, this approach effectively achieves not only facial  
47 symmetry, particularly in the lower face, but also a more natural and normalized facial form. This novel  
48 approach, aligning with soft-tissue-driven planning principles, shows promise in surpassing traditional methods,  
49 potentially leading to enhanced facial outcomes and patient satisfaction in orthognathic surgery.

50

51 **Keywords:** Craniofacial abnormalities, Orthognathic surgery, Cephalometry, Facial asymmetry, Deformity

## 52    **2    Introduction**

53        Current orthognathic surgical planning follows a skeletal-driven approach.<sup>1-3</sup> It focuses on rectifying  
54 malocclusion and skeletal abnormalities, expecting optimal facial appearance to ensue. Within this framework,  
55 one can (1) trust achieving an optimal facial appearance through skeletal correction without ever simulating the  
56 soft tissue changes or (2) validate and potentially revising the skeletal plan by simulating the facial appearance  
57 using computer software. However, both tactics have limitations. On the one hand, expecting a normal facial  
58 appearance without simulating the soft-tissue deformation may overlook asymmetries within the facial soft-  
59 tissue envelope or atypical bone-to-soft-tissue relationships.<sup>4,5</sup> On the other hand, simulating the facial  
60 appearance after the planned skeletal correction often necessitates time-consuming iterations and multiple plan  
61 revisions, making the process less efficient.<sup>6-8</sup>

62        To address these limitations of the current skeletal-driven method, a soft-tissue-driven planning method has  
63 been proposed.<sup>9</sup> This approach estimates the necessary bone movements based on the optimal facial appearance,  
64 significantly enhancing both the efficiency and accuracy of the surgical plan.

65        While the accuracy in estimating an optimal facial appearance is critical for soft-tissue-driven planning,  
66 predicting this appearance before planning remains a significant challenge.<sup>9,10</sup> Existing methods predominantly  
67 rely on landmark-based estimations to project postoperative facial appearance, due to the difficulties in  
68 accurately rendering the three-dimensional (3D) facial surface using limited preoperative data. These methods  
69 typically involve initial predictions of landmark movements, followed by the reconstruction of facial surfaces  
70 using simple interpolation techniques, such as thin plate spline (TPS) interpolation.<sup>11</sup> Previous research has  
71 employed the partial least square (PLS) method<sup>12</sup> in a supervised learning approach, using postoperative  
72 landmarks as the target.<sup>13-15</sup> These studies have incorporated data on types of deformities and surgical  
73 operations, along with preoperative and postoperative landmarks. However, the supervised approach has  
74 limitations, as it is trained to predict postoperative outcomes without guaranteeing an optimal outcome. Given  
75 that postoperative faces may still present residual deformities or asymmetries,<sup>16</sup> relying solely on this data for  
76 training can be problematic. Ideally, optimal facial landmarks should adhere to universally accepted aesthetic  
77 norms represented by the distribution of cephalometric values within normal subjects while accounting for  
78 patient-specific characteristics.

79

80       The ultimate goal is to accurately estimate the optimal facial appearance for soft-tissue-driven planning,  
81       which can be achieved in two phases. The first phase involves estimating patient-specific optimal facial  
82       landmarks, and the second involves reconstructing an optimal facial surface based on these landmarks.

83       This study primarily focused on the first phases, addressing the significant challenge of estimating patient-  
84       specific optimal facial landmarks. The objectives were twofold: firstly, to develop an algorithm capable of  
85       accurately predicting the optimal position of facial landmarks in patients with jaw deformities; and secondly, to  
86       validate this methodology. Facial landmarks were defined as being in an optimal position when they satisfy  
87       three key outcomes: (1) perfect lower facial *symmetry*, (2) a normal facial *form*, and (3) preservation of the  
88       patient's unique phenotype.

## 89 **3 Materials and Methods**

90 This study was conducted at Houston Methodist Research Institute (HMRI, Houston, Texas) and Rensselaer  
91 Polytechnic Institute (RPI, Troy, New York). The in-silico investigation utilized de-identified retrospective  
92 maxillofacial patient data. The Institutional Review Board (IRB) of HMRI approved the study—IRB#  
93 MOD00005116.

94 The first aim of the study was to devise an optimization algorithm to estimate the optimal facial landmarks  
95 for individuals with jaw deformities. The second aim was to validate the algorithm. To achieve both these  
96 objectives, the investigators relied on maxillofacial imaging data drawn from two distinct populations: (1) a  
97 cohort of jaw deformity patients and (2) a normal subject group.

98 Patients were included in the jaw deformity dataset if (1) they had undergone orthognathic surgery in the  
99 upper jaw, lower jaw, or both; (2) they had preoperative and postoperative imaging records in our virtual  
100 surgical simulation (VSP) software, AnatomicAligner (HMRI, Houston, Texas);<sup>17</sup> and (3) the surgical plan had  
101 been formulated following a skeletal-driven tactic.

102 Subjects were included in the normal group if (1) they had no facial deformity and (2) had records in our  
103 VSP software. The VSP software files of each patient contained three-dimensional models of the facial soft-  
104 tissues, and well as their cephalometric landmarks (Table1). Infants and children were excluded from both  
105 groups.

106 To ensure accurate and consistent evaluation of cephalometric measurements, the 3D facial models of  
107 patients and normal subjects were aligned to their sagittal, coronal, and axial planes. The aforementioned frame  
108 of reference was calculated by the automatic function present in the AnatomicAligner software.<sup>18</sup> Before the  
109 study began, the jaw deformity cohort was randomly split into two equal groups. The first group was utilized to  
110 fine-tune the optimization algorithm, while the second served to validate it.

### 111 **3.1 Optimal Landmark Prediction**

112 Our method for predicting optimal facial landmarks incorporates a combination of *symmetrization* process  
113 and *weighted optimization* approach. To select the appropriate measurements for the algorithm, the literature  
114 was searched to find useful published facial (i.e., soft tissue) cephalometric measurements.<sup>19–23</sup> These  
115 measurements were divided into two categories: facial *symmetry* and facial *form*.

116

### 117 **3.1.1 Symmetrization**

118 The *symmetrization* process began with the use of facial *symmetry* measurements. These measurements were  
119 subdivided into two types: *bilateral point differences* and *midpoint deviations from the sagittal plane*. The  
120 assessment of bilateral point differences involved the calculation of absolute differences in the symmetry of  
121 bilateral points across the vertical, transverse, and anteroposterior dimensions. On the other hand, the  
122 assessment of *midpoint deviations from the sagittal plane* measured the absolute perpendicular distances  
123 between jaw midline landmarks and the sagittal plane, which included the *Sn* landmark. *Symmetry*  
124 measurements are crucial for assessing the alignment and symmetry of facial features in relation to the central  
125 plane of the face.

126 Aiming for perfect symmetry, the *symmetrization* process adjusts bilateral points towards their average  
127 positions, effectively reducing the bilateral point differences to zero. Similarly, midpoint deviations from the  
128 sagittal plane are also aligned to zero, establishing a symmetrical baseline. In total, 12 facial *symmetry*  
129 measurements were included. (Table 2)

130

### 131 **3.1.2 Weighted Optimization for Facial Form Measurements**

132 To ascertain the most relevant facial *form* measurements for the algorithm, a comparative test was conducted.  
133 This analysis juxtaposed the averages and distributions of each facial *form* measurement across three distinct  
134 groups: (1) patients with jaw deformities, (2) those postoperative corrections, and (3) normal subjects. Only  
135 those *form* measurements that were altered by orthognathic surgery and subsequently aligned with the  
136 distributions of the normal group were incorporated into the optimization approach.

137 Facial *form* measurements were subdivided by type: *angle*, *ratio*, and *length*. This categorization was crucial  
138 because each type of measurement has its distinct units and scales. Combining them without differentiation in  
139 our model might introduce bias. To mitigate this, specific weights were allocated to each type. The weighting  
140 factor ( $\lambda_i$ ) was determined through a rigorous iterative empirical process, refining the weights until the corrected  
141 cephalometric values closely matched the distribution found in the normal subject group. Data from both patient  
142 and normal subject groups were used in this determination. *Angle* measurements received a weight of 0.8, *ratio*  
143 a weight of 0.05, *length* a weight of 0.2. A total of 6 facial *form* measurements were included. (Table 2) A  
144 statistical comparison between the postoperative dataset and the normal subject dataset used for the selection is  
145 presented at Section 3.3 (statistical analysis).

146 The *weighted optimization* approach considered the following assumption. Given the uniqueness of each

147 human face, its facial *form* measurements should not conform to the average of a population. Instead, optimal  
148 landmarks are those that (1) generate facial *form* measurements that are within the distribution of normal and (2)  
149 preserve the patient's phenotype.

150 This approach computed the necessary displacement to rectify distorted landmarks by minimizing the  
151 objective function outlined in Equation 1.

$$d_{opt} = \underset{\mathbf{d} \in \mathbb{R}^3}{\operatorname{argmin}} \left( \sum_{i \in CM} \lambda_i \frac{(M_i(\mathbf{x} + \mathbf{d}) - \mu_i)^2}{\sigma_i^2} + \lambda_{L2} \|\mathbf{d}\|^2 \right) \quad (1)$$

152

153 In this equation,  $x$  represents the deformed facial landmark,  $d$  is the landmark displacement vector  
154 required for the optimization,  $M$  is the facial *form* measurement,  $CM$  is a set of facial *form* measurements  
155 (Table 2), and  $d_{opt}$  is the optimal landmark displacement.  $\mu$  and  $\sigma$  are the mean and standard deviation of  
156 facial *form* values of the normal subject group.  $\lambda_i$  is the weighting factor for the facial *form* type (*angle*, *ratio*,  
157 and *length*).  $\lambda_{L2}$  is the weighting factor for the  $L2$  regularization term that preserves patient-specificity. Its  
158 value  $\lambda_{L2}=1.0$  was determined through an empirical process like the one used to determine  $\lambda_i$ .

159 The gradient descent method was employed to minimize the objective function and find the optimal  
160 displacement vector  $d$ . The optimal facial landmarks were then predicted by applying the estimated  
161 displacement vectors  $d$  to the corresponding deformed landmarks. During the optimization, the landmarks  
162 corresponding to the upper face (Gb', Prn, CM, and Sn) were assumed fixed because they are not directly  
163 affected by orthognathic surgery.

164

### 165 3.1.3. Optimal Landmark Prediction

166 Sequential application of *symmetrization* and *weighted optimization* failed to achieve symmetry between the  
167 right and left cheilions—vertical, transverse, and anteroposterior cheilion symmetry. To solve this problem, a  
168 three-step approach was implemented. In the first step, the displacement vectors for all landmarks, excluding the  
169 right and left cheilions, were calculated by sequentially applying *Symmetrization* and *weighted optimization*. In  
170 the second step, the movement of the cheilions was inferred based on the movements of the other landmarks  
171 through Thin-Plate Spline (TPS) interpolation. The third step focused solely on the right and left cheilions,  
172 computing their displacement vectors to achieve vertical, transverse, and anteroposterior symmetry by  
173 *symmetrization*, while keeping the positions of other landmarks fixed.



## 174 3.2 Validation

175 To validate the newly proposed method, two hypotheses were formulated: (1) the new approach would yield  
176 facial landmarks that have perfect lower facial *symmetry* and normal facial *form*; (2) the new methodology  
177 would render superior results compared with outcomes obtained through established skeletal-driven planning.

178 A methodical procedure was employed to examine the first hypothesis, specifically whether the approach  
179 results in facial landmarks that have perfect lower facial *symmetry* and normal facial *form*. The procedure began  
180 with predicting patient-specific optimal facial landmarks for the dataset of patients exhibiting facial deformities.  
181 Subsequently, cephalometric measurements derived from these estimated facial landmarks were juxtaposed with  
182 those extracted from a dataset of normal subjects.

183 To scrutinize the second hypothesis, a comparative analysis was conducted between cephalometric  
184 measurements from two groups: (1) faces refined through the proposed method and (2) postoperative faces  
185 resulting from skeletal-driven planning. This comparative evaluation aimed to ascertain whether the proposed  
186 methodology offered advantages over conventional skeletal-driven planning.

187 In addition to testing the study hypotheses, a post-hoc test was conducted to compare the cephalometric  
188 measurements of (1) postoperative faces acquired through traditional skeletal-driven planning with those of (2)  
189 normal individuals. The purpose of this comparison was to support our assertion that skeletal-driven planning  
190 does not lead to soft-tissue normalization.

## 191 3.3 Statistical Analysis

192 For the development and validation of the new method, a rigorous statistical analysis was conducted to  
193 scrutinize the variations in the distribution of cephalometric measurements among three distinct groups:  
194 optimized preoperative, postoperative, and normal subjects. Traditional analytical approaches such as ANOVA  
195 or Kruskal-Wallis tests were deemed unsuitable for this inquiry due to the amalgamation of paired and unpaired  
196 comparisons present in the datasets. Consequently, a series of comparisons between each group was undertaken.  
197 Considering the multitude of comparisons intrinsic to this analysis, a corrected p-value of 0.017 was necessary  
198 to uphold an overall significance of 0.05. This adjustment was calculated employing the Bonferroni correction  
199 to counteract the risk of Type I error arising from multiple comparisons.

200

201 In this study, the *preoperative* and *postoperative* groups were paired, belonging to the same patients, the  
202 normal subject group was unmatched (it was a separate group of individuals). For the comparison between

203 paired groups, each distribution was first assessed for normality. If both groups exhibited a normal distribution,  
204 a paired t-test was performed. However, if one or both groups did not follow a normal distribution, a Wilcoxon  
205 signed-rank test was used instead.

206 For the comparison between unpaired groups (between patient group and normal subject group), the  
207 normality of the distributions for each group was initially examined. In cases where the distributions showed  
208 normality, Levene's test was further employed to verify the homogeneity of variances. If a significant difference  
209 in variances was detected, Welch's t-test was applied. Otherwise, Student's t-test was utilized. When one or both  
210 groups did not demonstrate normal distribution, the Mann-Whitney U test was employed for comparison.

211

## 212 **4 Results**

213 The deformity dataset consisted of 60 patients. Their mean age was 23.3 years, SD 6.9. Thirty-eight were  
214 females and 22 males. The normal subject group had 48 patients. Their mean age was 21.7 years, SD 2.5.  
215 Twenty-eight were females and 20 males.

216 As indicated in Table 3, the comparison of cephalometric measurements of the predicted optimal landmark  
217 group with those of normal subject group shows statistically significant differences for all symmetry-related  
218 measurements. Conversely, no statistically significant differences were observed for facial form measurements.  
219 This finding indicated that the predicted landmarks exhibited perfect symmetry, unlike those in the normal  
220 subject. It validated the first hypothesis, demonstrating that the proposed approach produces perfect lower face  
221 symmetry while maintaining normal facial form.

222 Similarly, when comparing the cephalometric measurements obtained from the predicted optimal  
223 landmarkgroup with those of postoperative patients (as presented in Table 4), it was revealed that all symmetry  
224 measurements exhibited statistically superior results in the predicted optimal landmark. Additionally, the facial  
225 form measurements revealed no significant differences among the predicted optimal landmark group,  
226 postoperative group, and normal subject group.

227 This outcome provides confirmation for our second hypothesis, proving that the new methodology yields  
228 superior results compared to outcomes achieved through established bone-driven planning, especially in the  
229 context of enhancing facial symmetry without the degradation of facial form.

230 The post-hoc comparison between the cephalometric measurements of postoperative patients and those of  
231 normal subjects showed that that 5 out of 14 measurements were statistically worse in the postoperative group.  
232 Again, all statistically significant differences in cephalometric measurements pertain to facial symmetry. This  
233 outcome confirms our assertion that bone-driven planning does not lead to complete soft-tissue normalization,  
234 particularly in facial symmetry.

235 Figures 1 and 2 provide visual representations of these findings. Figure 1 displays the distribution of each  
236 measurement across all groups, including cephalometric measurements of the preoperative group to illustrate  
237 changes following surgery. Figure 2 presents an example case demonstrating the estimated optimal landmarks.

238

239

## 240 **5 Discussion**

241 In this study, the researchers have pioneered an innovative approach for the prediction of optimal facial  
242 landmarks in individuals suffering from jaw deformities. The **key findings** of the study are significant in several  
243 aspects. Firstly, the developed methodology achieves facial symmetry, particularly in the lower face, while  
244 ensuring that the facial appearance remains patient-specific and normal. Secondly, this novel approach  
245 potentially surpasses traditional bone-driven planning methods in delivering enhanced facial outcomes, with  
246 notable improvement in symmetry.

247 Furthermore, a post-hoc analysis comparing cephalometric measurements of *postoperative patients* to those  
248 of *normal subjects* highlighted that traditional bone-centric planning often falls short in achieving complete soft-  
249 tissue normalization, especially in terms of facial *symmetry*.

250 The **clinical relevance** of this project lies in its challenge to the current skeletal-centric paradigm in  
251 orthognathic surgery. The prevalent skeletal-centric approach emphasized the correction of malocclusion and  
252 skeletal anomalies, with the expectation that aesthetically pleasing facial appearance would ensue. During  
253 planning, skeletal-centric method is implemented in two distinct ways. Firstly, some clinicians assume that  
254 correcting skeletal deformities alone will result in optimal facial aesthetics, hence they do not simulate the soft  
255 tissue changes. Secondly, other clinicians employ computer algorithms to predict the facial outcome post-  
256 skeletally corrective procedures, thus substantiating the skeletal plan.

257 Despite the everyday use of these methodologies, practical limitations are evident. Relying solely on skeletal  
258 adjustments without visualizing the soft tissue changes could miss asymmetries in the facial soft tissue or  
259 atypical correlations between bone structure and adjacent soft tissues.<sup>4,5</sup> Conversely, the employment of facial  
260 simulation software in the planning stage, while beneficial for visualizing postoperative outcomes, often  
261 necessitated labor-intensive iterative processes and multiple revisions of the surgical plan. This dichotomy  
262 highlights the inherent complexities and challenges in achieving a harmonious balance between skeletal  
263 correction and desirable facial aesthetics in orthognathic surgery.

264 The research group proposed a novel soft-tissue-driven planning method for orthognathic surgery,<sup>9</sup> which  
265 could potentially resolve the aforementioned issues. This method began by simulating an optimal facial  
266 appearance and then calculated the necessary skeletal framework to support the overlying soft tissues,  
267 considering their thickness and composition. The process culminates in guiding the three-dimensional alignment  
268 of the jaw segments to match the ideal skeletal framework closely. This step goes beyond mere aesthetic  
269 alignment; it ensures the maintenance of normal occlusion and jaw function for the patient. By emphasizing the

270 role of soft tissue in surgical planning, the soft-tissue-driven method aims to achieve outcomes that are not only  
271 aesthetically pleasing but also functionally sound. This represents a shift from traditional methods that might  
272 focus primarily on the skeletal structure, offering a more patient-centric and comprehensive approach to  
273 orthognathic surgery.

274 This study tackles the first stage necessary for applying a soft-tissue-driven approach, aiming to simulate  
275 the optimal facial appearance of patients. This task involves two key steps: firstly, repositioning deformed facial  
276 landmarks to an ideal position, and secondly, rendering the optimal soft-tissue surface. In this paper, we propose  
277 a solution for the initial step, with plans to address the second step in a subsequent study.

278 Rather than relocating facial landmarks to positions typical of an average population, our weighted  
279 optimization approach moves deformed facial landmarks to appropriate positions while preserving each patient's  
280 unique characteristics. Our method differentiates between cephalometric measurements for evaluating symmetry  
281 and those for assessing facial *form*. The method aims at perfect lower facial *symmetry* but avoids average facial  
282 *form*. Although achieving perfect lower facial *symmetry* is not surgically feasible, creating a symmetrical  
283 template for planning is valuable. It may decrease the likelihood of postoperative asymmetry.

284 On the other hand, an average facial *form* might not be suitable for all patients. Typically, cephalometric  
285 measurements in a normal population are distributed around a mean value. By limiting the movement of facial  
286 landmarks to positions that enter the normal range, but are not necessarily aligned with the means, one can  
287 maintain the patient's phenotype and enhance the likelihood that the surgery will be feasible.

288 Despite the promising results, our study has **limitations**. Firstly, the accuracy and generalizability of the  
289 approach depends on the characteristics of the normal group population. To enhance the applicability of the  
290 method, future research will focus on expanding the normative database to include a more diverse population,  
291 considering factors such as gender, age, and ethnicity.

292 Another limitation lies in the heavy reliance on cephalometric measurements as the primary measure for the  
293 optimal landmark prediction. While cephalometric measurements provide valuable information for assessing  
294 facial aesthetics, they have inherent limitations in capturing the complex multidimensional nature of facial  
295 aesthetics. To overcome this limitation, future studies could explore the integration of additional measurements  
296 utilizing three-dimensional information.

297 Finally, while in the study, the distributions of cephalometric measurements in the *estimated preoperative*  
298 *group* are within those of the *postoperative group* (as shown in Figure 1), the study does not prove that the  
299 *predicted optimal facial appearances* are surgically attainable for individual patients.

300

301       The **future direction** of this project involves developing all the necessary technology for implementing soft-  
302 tissue-driven planning. This includes: (1) rendering an optimal facial appearance based on optimized landmarks,  
303 (2) calculating the necessary skeletal framework to support the overlying soft tissues, and (3) guiding the three-  
304 dimensional alignment of the jaw segments to closely match the idealized skeletal framework.

305       In **conclusion**, the novel approach for predicting optimal facial landmarks achieved an optimal balance  
306 between normalization of facial deformities and preservation of individual characteristics. The new method  
307 signifies a substantial advancement in optimal face prediction for soft-tissue-driven surgical planning, holding  
308 the promise of enhancing surgical outcomes and patient satisfaction.

### 309   **Declarations**

310   **Funding:** This work was partially supported by NIH under awards R01 DE021863

311   **Competing interests:** None.

312   **Ethical approval:** The study was approved by the institutional review boards of Houston Methodist Hospital  
313 and Research Institute (IRB#: MOD00005116)

314   **Patient consent:** Not applicable.

315

316

317

318

319

320

321

322 **6 References**

- 323 1. Seo HJ., Choi Y-K. Current trends in orthognathic surgery. *Arch Craniofac Surg* 2021;22(6):287.
- 324 2. Choi J-W., Lee JY., Choi J-W., Lee JY. Treatment Strategy for Class II Orthognathic Surgery: Orthodontic  
325 Perspective. *The Surgery-First Orthognathic Approach: With Discussion of Occlusal Plane-Altering*  
326 *Orthognathic Surgery* 2021:71–100.
- 327 3. Hammoudeh JA., Howell LK., Boutros S., Scott MA., Urata MM. Current status of surgical planning for  
328 orthognathic surgery: traditional methods versus 3D surgical planning. *Plast Reconstr Surg Glob Open*  
329 2015;3(2).
- 330 4. Kim D., Kuang T., Rodrigues YL., Gateno J., Shen SGF., Wang X., et al. A new approach of predicting facial  
331 changes following orthognathic surgery using realistic lip sliding effect. *Medical Image Computing and*  
332 *Computer Assisted Intervention–MICCAI 2019: 22nd International Conference, Shenzhen, China, October*  
333 *13–17, 2019, Proceedings, Part V 22*. Springer; 2019. p. 336–44.
- 334 5. Bell WH., Ferraro JW. Modern practice in orthognathic and reconstructive surgery. *Plast Reconstr Surg*  
335 1993;92(2):362.
- 336 6. Ma L., Xiao D., Kim D., Lian C., Kuang T., Liu Q., et al. Simulation of postoperative facial appearances via  
337 geometric deep learning for efficient orthognathic surgical planning. *IEEE Trans Med Imaging*  
338 2022;42(2):336–45.
- 339 7. Schendel SA., Jacobson R., Khalessi S. 3-dimensional facial simulation in orthognathic surgery: is it  
340 accurate? *Journal of Oral and Maxillofacial Surgery* 2013;71(8):1406–14.
- 341 8. Rokhshad R., Keyhan SO., Yousefi P. Artificial intelligence applications and ethical challenges in oral and  
342 maxillo-facial cosmetic surgery: a narrative review. *Maxillofac Plast Reconstr Surg* 2023;45(1):14.
- 343 9. Fang X., Kim D., Xu X., Kuang T., Lampen N., Lee J., et al. Soft-Tissue Driven Craniomaxillofacial Surgical  
344 Planning. *International Conference on Medical Image Computing and Computer-Assisted Intervention*.  
345 Springer; 2023. p. 186–95.
- 346 10. Modabber A., Baron T., Peters F., Kniha K., Danesh G., Hölzle F., et al. Comparison of soft tissue  
347 simulations between two planning software programs for orthognathic surgery. *Sci Rep* 2022;12(1):5013.
- 348 11. Keller W., Borkowski A. Thin plate spline interpolation. *J Geod* 2019;93:1251–69.
- 349 12. Wold H. Estimation of principal components and related models by iterative least squares. *Multivariate*  
350 *Analysis* 1966:391–420.

- 351 13. Suh H-Y., Lee S-J., Lee Y-S., Donatelli RE., Wheeler TT., Kim S-H., et al. A more accurate method of  
352 predicting soft tissue changes after mandibular setback surgery. *Journal of Oral and Maxillofacial Surgery*  
353 2012;70(10):e553–62.
- 354 14. Yoon K-S., Lee H-J., Lee S-J., Donatelli RE. Testing a better method of predicting postsurgery soft tissue  
355 response in Class II patients: a prospective study and validity assessment. *Angle Orthod* 2015;85(4):597–  
356 603.
- 357 15. Suh H-Y., Lee H-J., Lee Y-S., Eo S-H., Donatelli RE., Lee S-J. Predicting soft tissue changes after  
358 orthognathic surgery: the sparse partial least squares method. *Angle Orthod* 2019;89(6):910–6.
- 359 16. Ajmera DH., Hsung RT-C., Singh P., Wong NSM., Yeung AWK., Lam WYH., et al. Three-dimensional  
360 assessment of facial asymmetry in Class III subjects. Part 1: a retrospective study evaluating postsurgical  
361 outcomes. *Clin Oral Investig* 2022;26(7):4947–66.
- 362 17. Yuan P., Mai H., Li J., Ho DC-Y., Lai Y., Liu S., et al. Design, development and clinical validation of  
363 computer-aided surgical simulation system for streamlined orthognathic surgical planning. *Int J Comput*  
364 *Assist Radiol Surg* 2017;12:2129–43.
- 365 18. Gateno J., Jajoo A., Nicol M., Xia JJ. The primal sagittal plane of the head: a new concept. *Int J Oral*  
366 *Maxillofac Surg* 2016;45(3):399–405.
- 367 19. Naini FB., Gill DS. Facial aesthetics: 2. Clinical assessment. *Dent Update* 2008;35(3):159–70.
- 368 20. Jagadish Chandra H., Ravi MS., Sharma SM., Rajendra Prasad B. Standards of facial esthetics: an  
369 anthropometric study. *J Maxillofac Oral Surg* 2012;11:384–9.
- 370 21. Oh J., Han JJ., Ryu S-Y., Oh H-K., Kook M-S., Jung S., et al. Clinical and cephalometric analysis of facial  
371 soft tissue. *Journal of Craniofacial Surgery* 2017;28(5):e431–8.
- 372 22. Eggerstedt M., Rhee J., Urban MJ., Mangahas A., Smith RM., Revenaugh PC. Beauty is in the eye of the  
373 follower: facial aesthetics in the age of social media. *Am J Otolaryngol* 2020;41(6):102643.
- 374 23. Reyneke JP., Ferretti C. Diagnosis and planning in orthognathic surgery. *Oral and Maxillofacial Surgery for*  
375 *the Clinician* 2021:1437–62.



376 **Figure Legends**

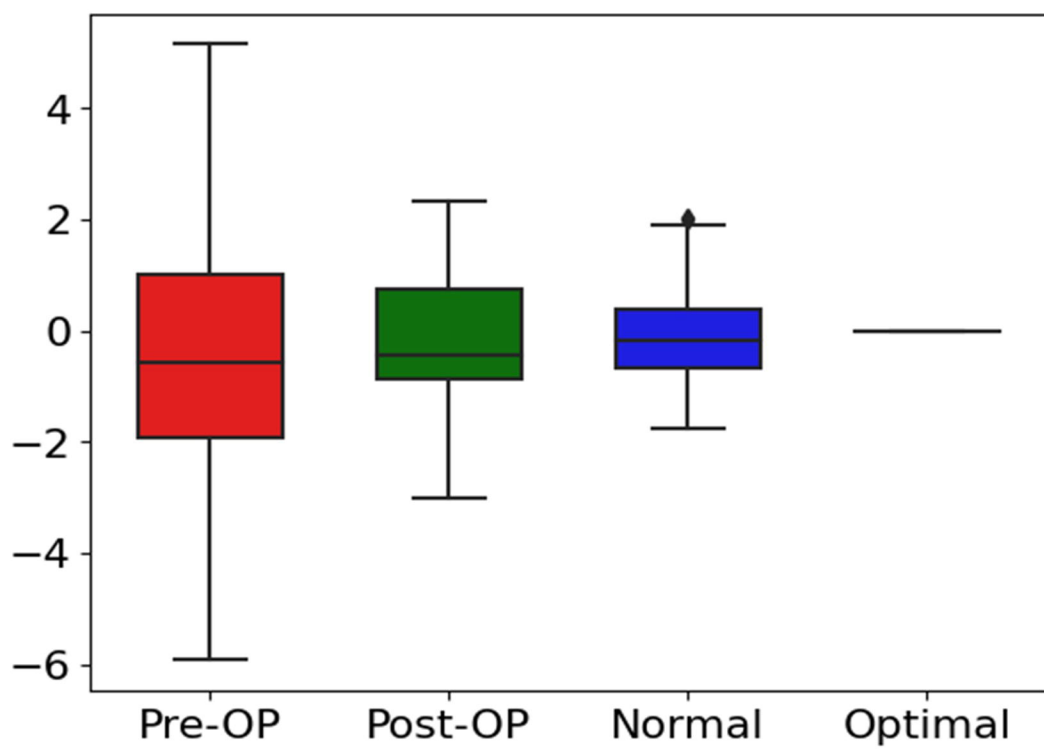
377

378 **Figure 1.** Box plots of cephalometric measurement of preoperative (Pre-OP; red), postoperative (Post-OP;  
379 green), normal group (blue), and predicted optimal landmarks (magenta).

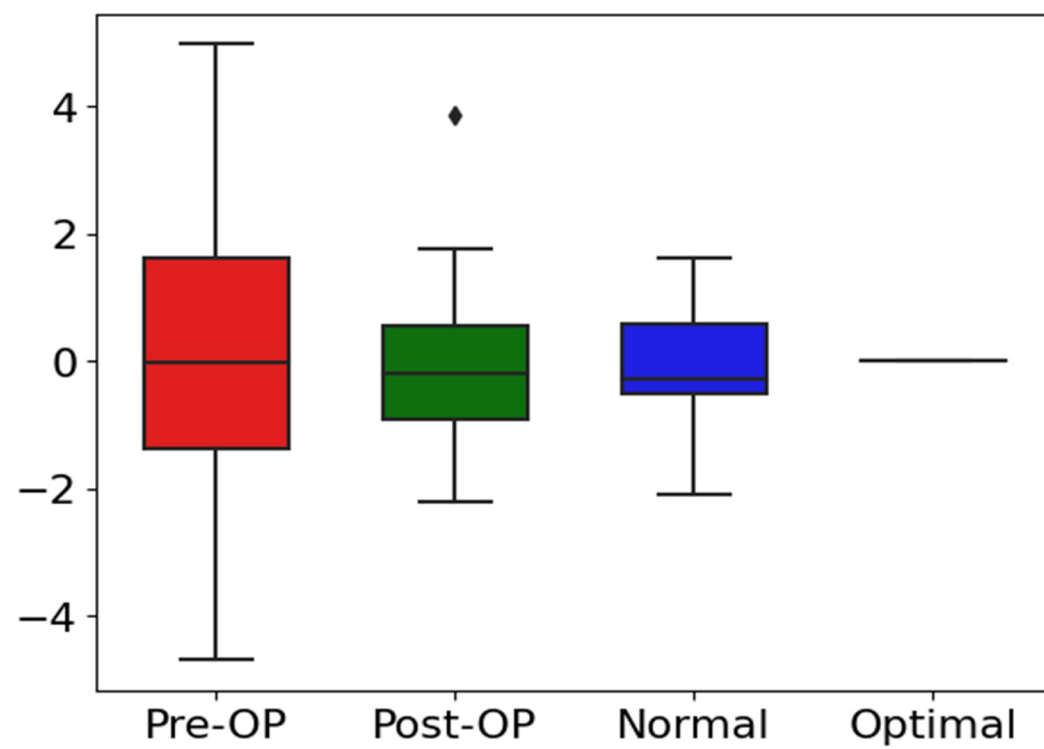
380

381 **Figure 2.** The positions of pre-operative (Pre-OP) and transformed landmarks in the frontal view (left), right  
382 profile view (middle), and left profile view (right) of randomly selected patient. Midline is defined as vertical  
383 line passing through the *subnasale*.

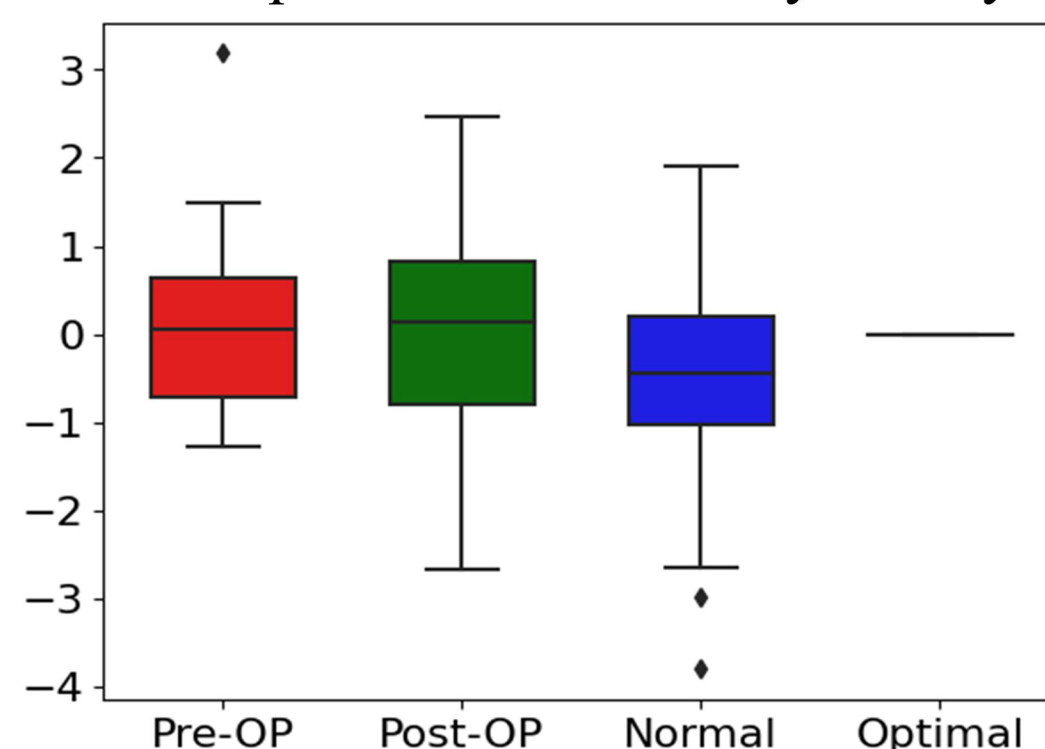
Vertical Cheilion Symmetry



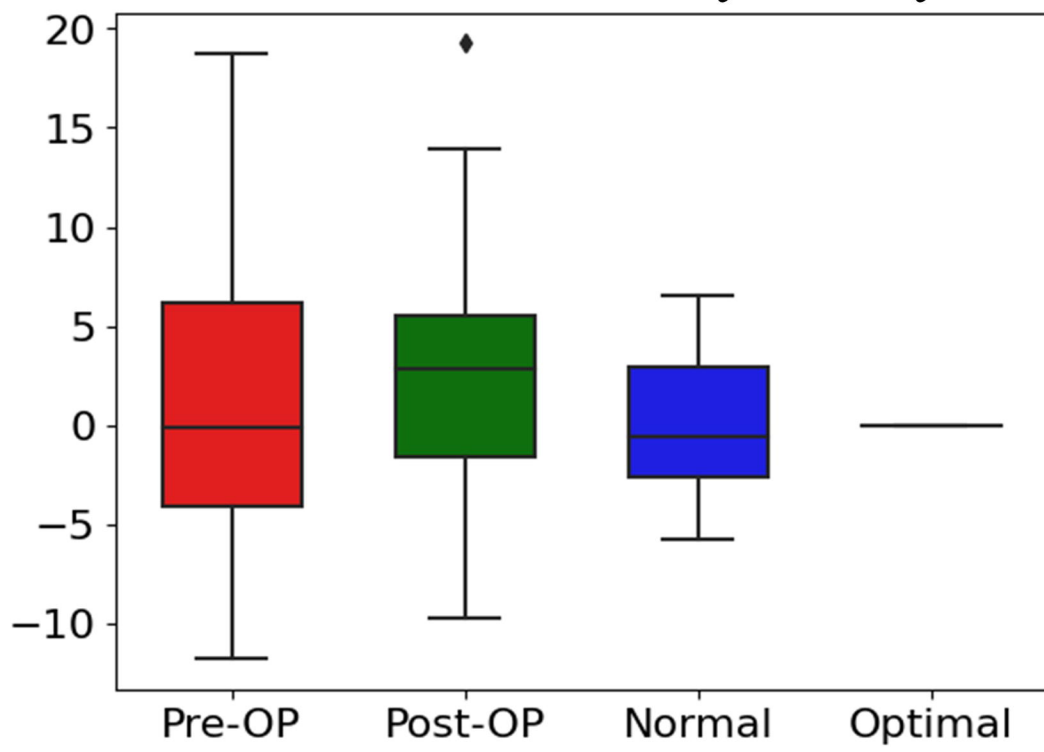
Transverse Cheilion Symmetry



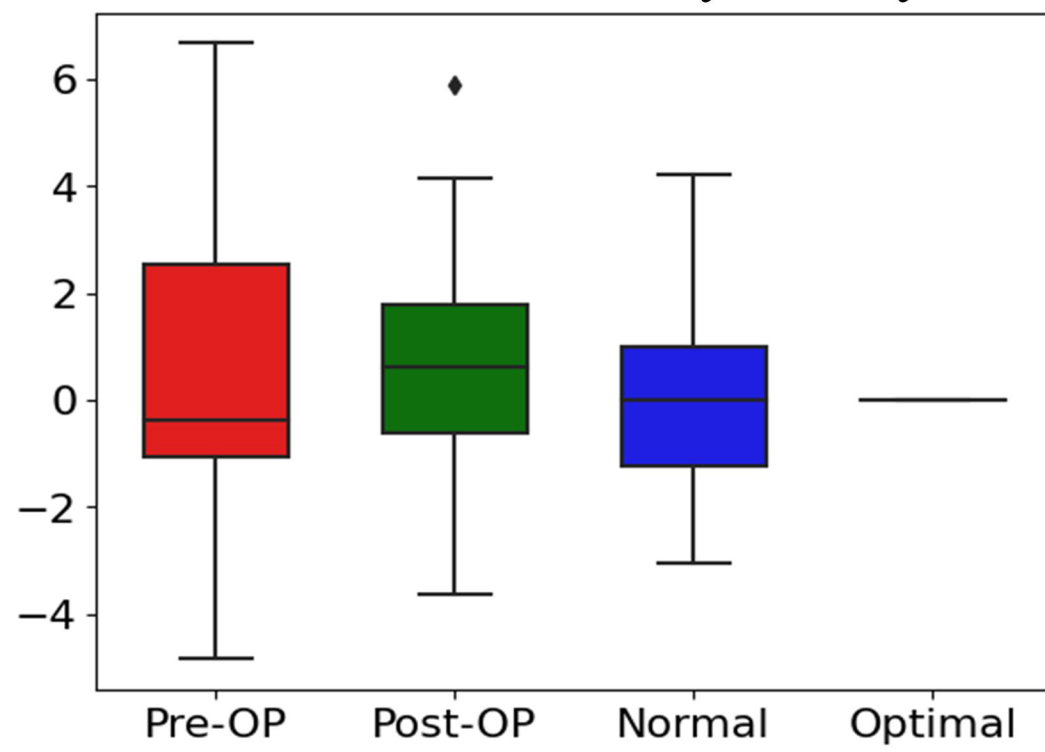
Anteroposterior Cheilion Symmetry



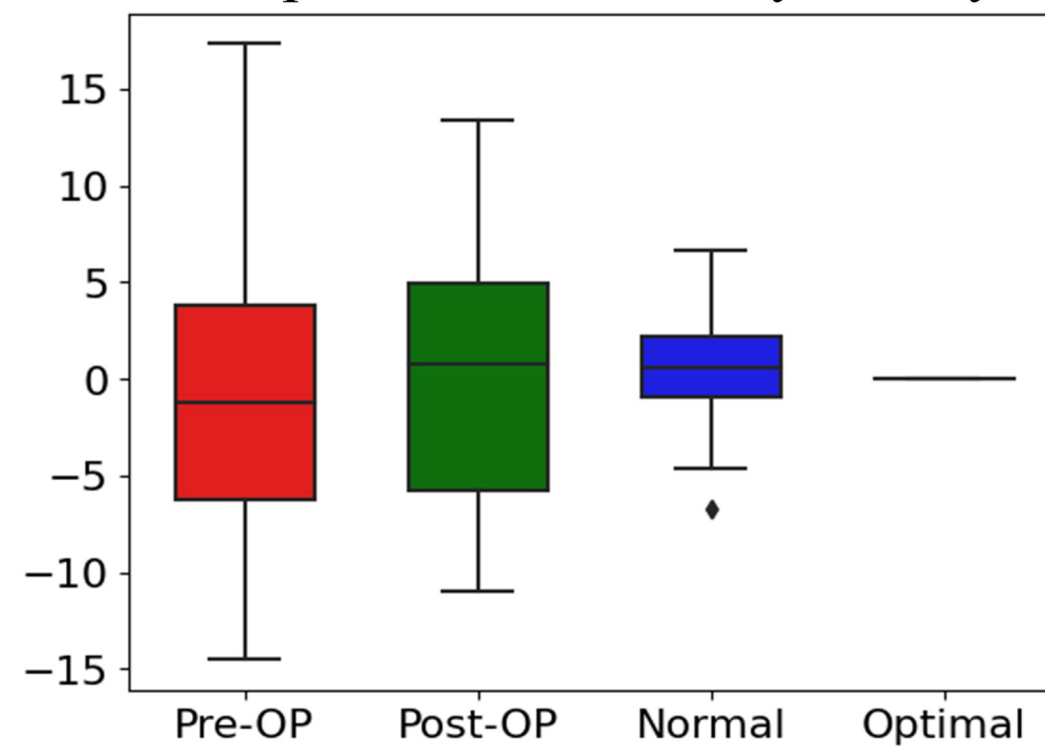
Vertical Gonion Symmetry



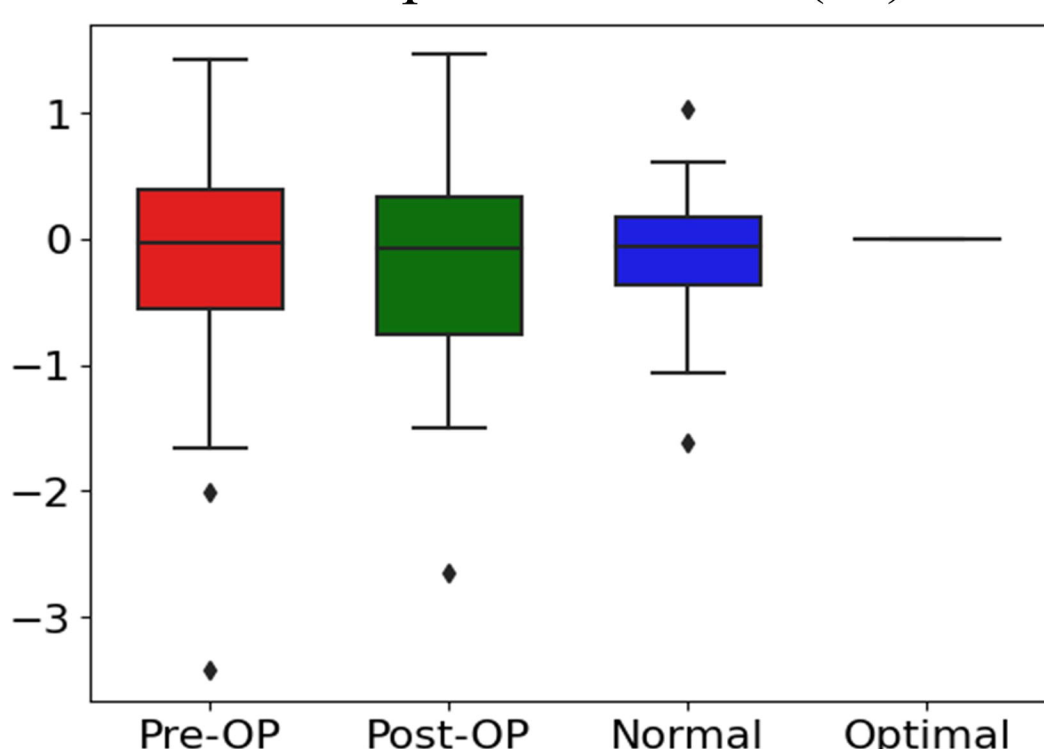
Transverse Gonion Symmetry



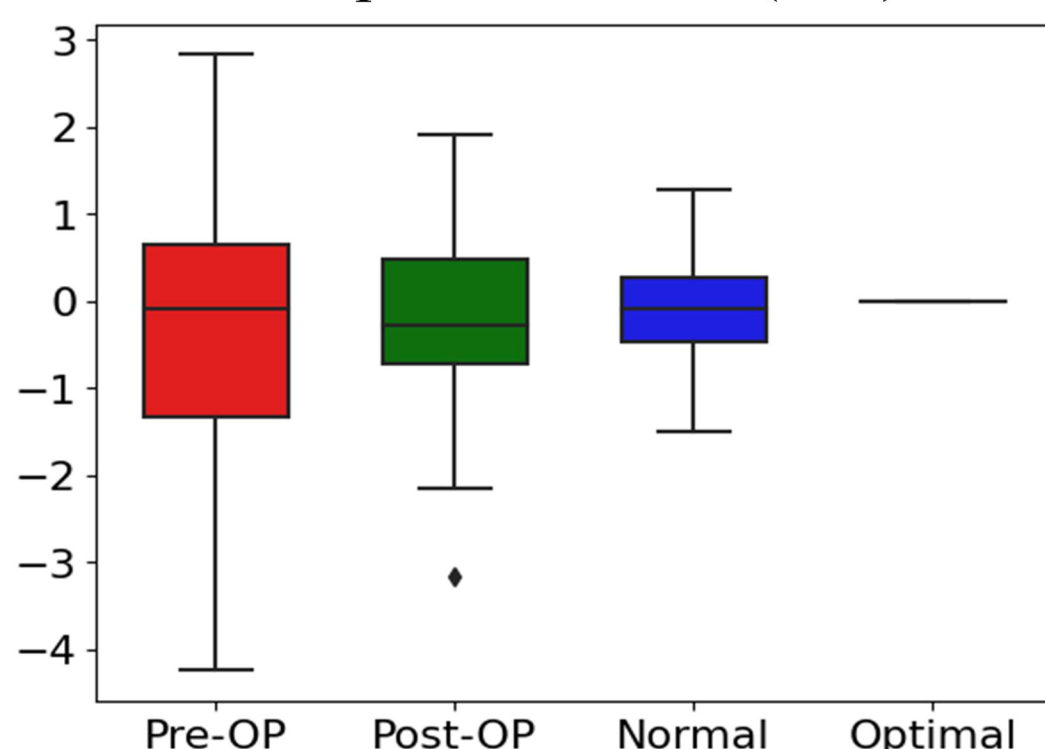
Anteroposterior Gonion Symmetry



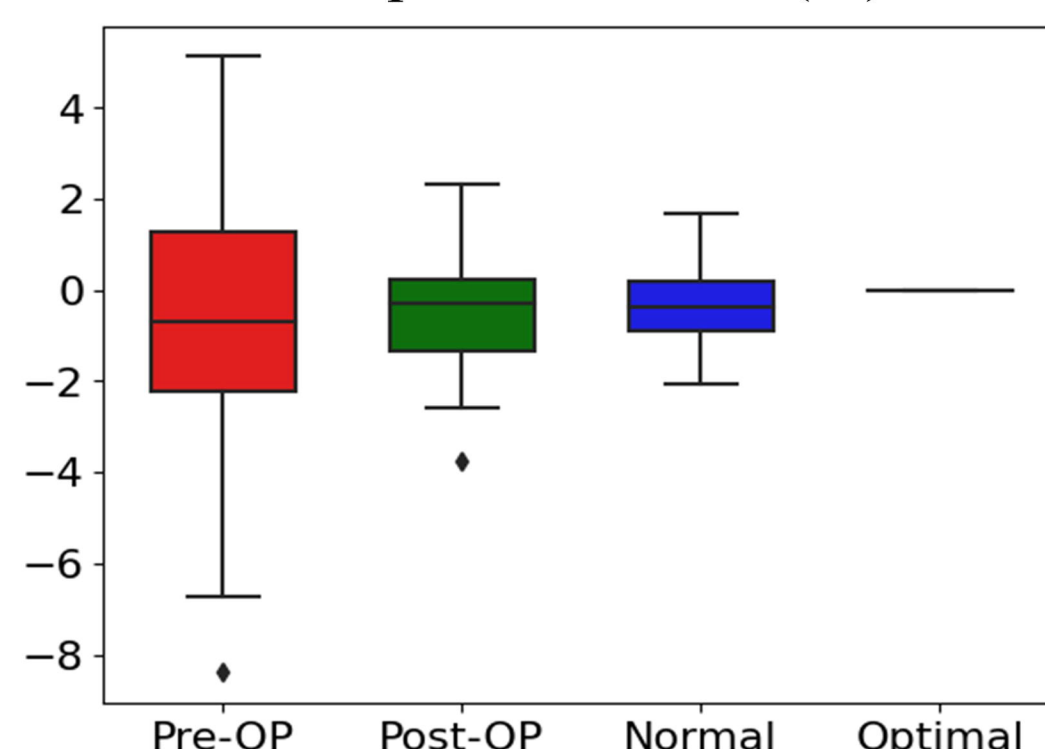
Midpoint deviation (Ls)



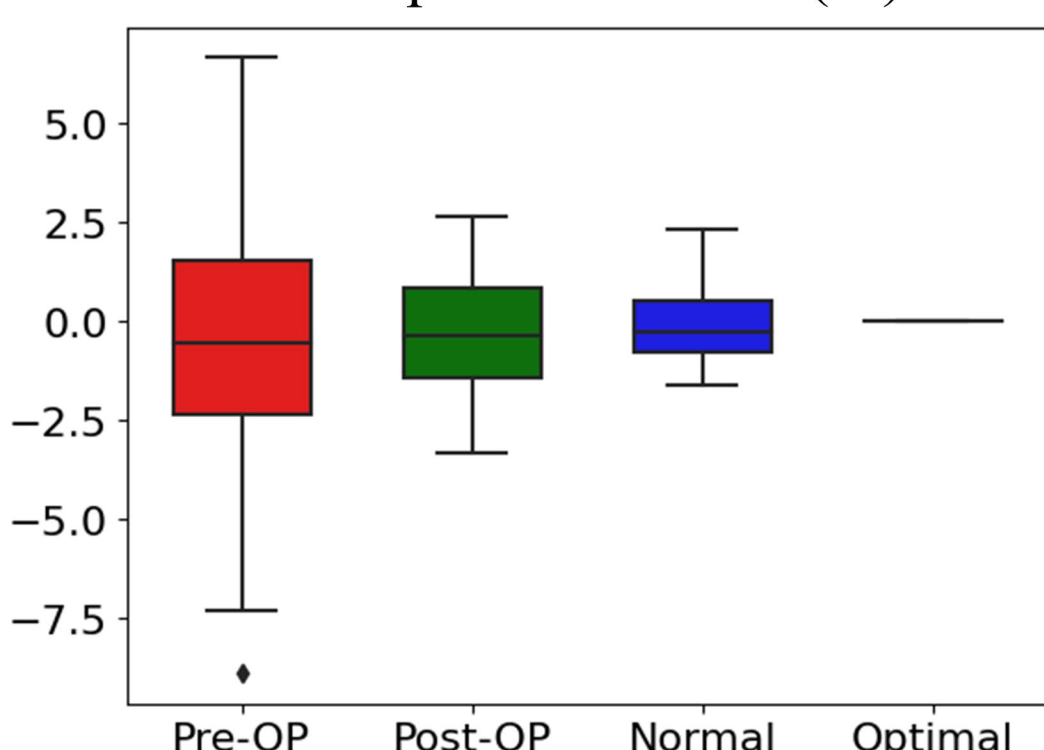
Midpoint deviation (Stm)



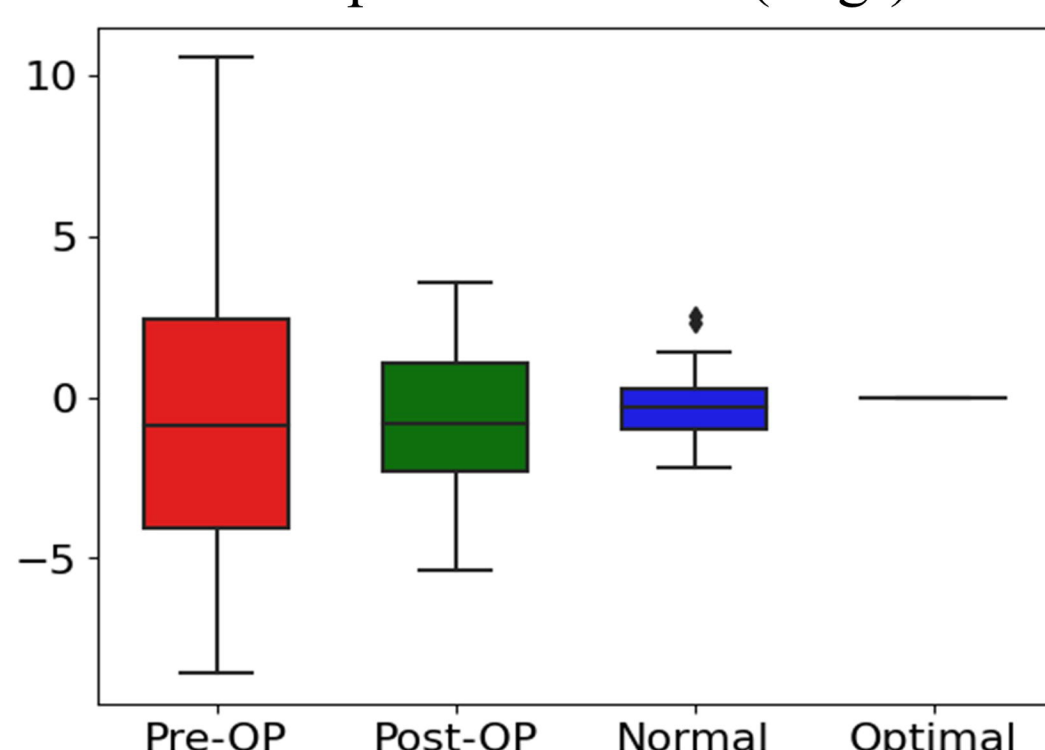
Midpoint deviation (Li)



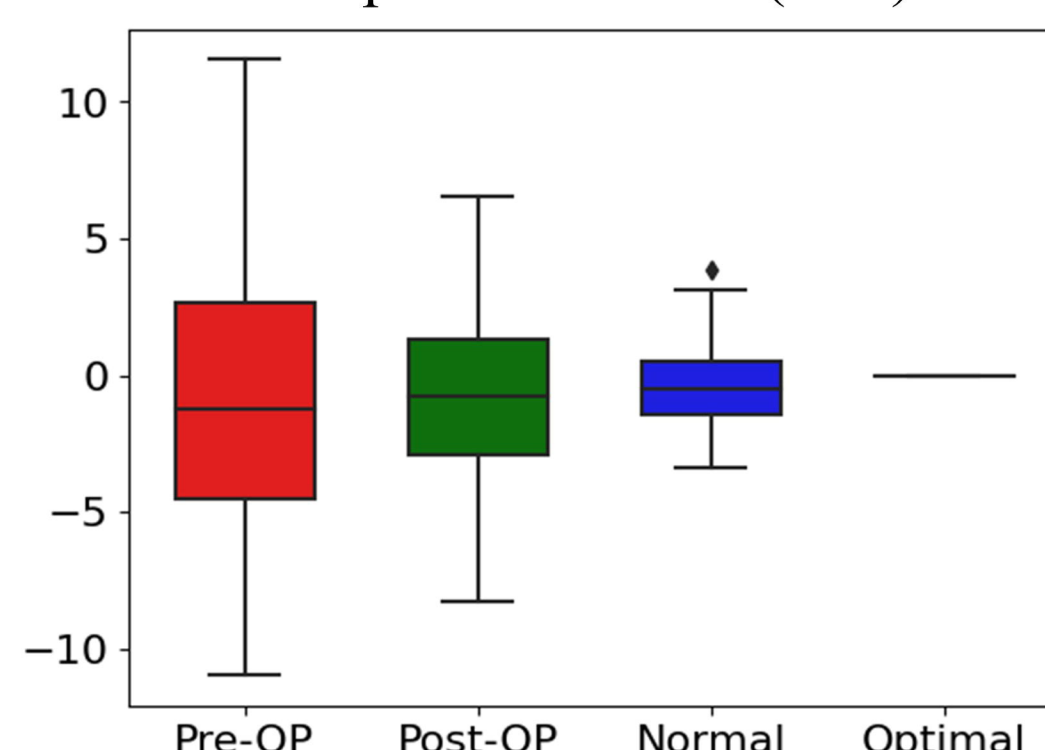
Midpoint deviation (Sl)



Midpoint deviation (Pog')



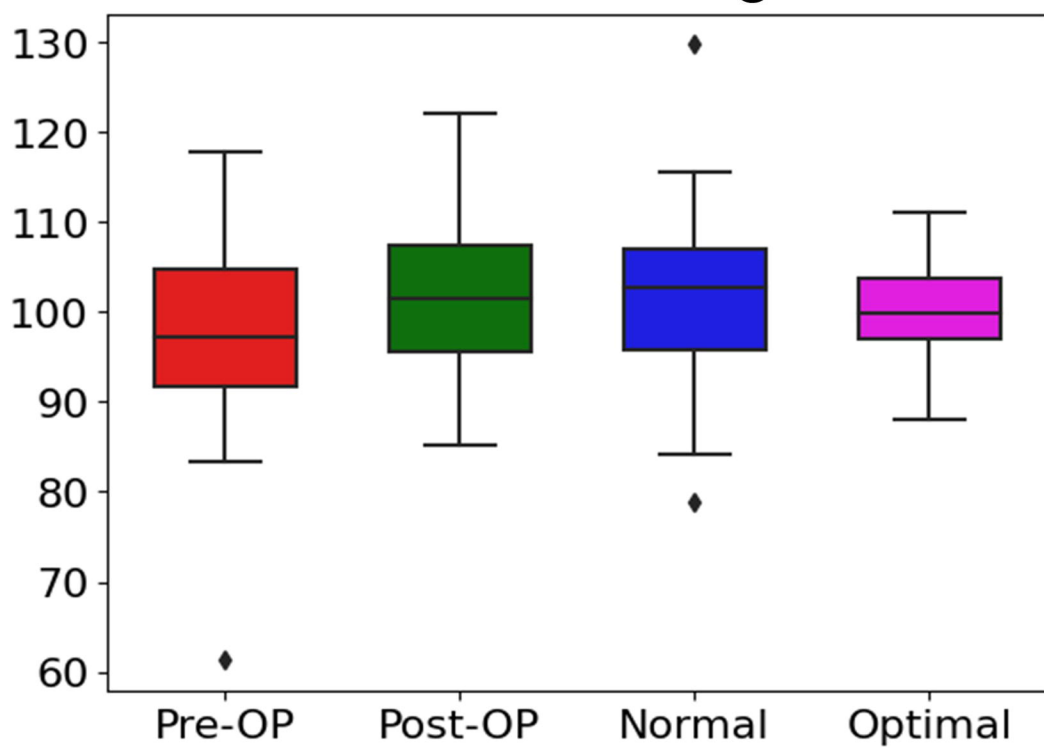
Midpoint deviation (Me')



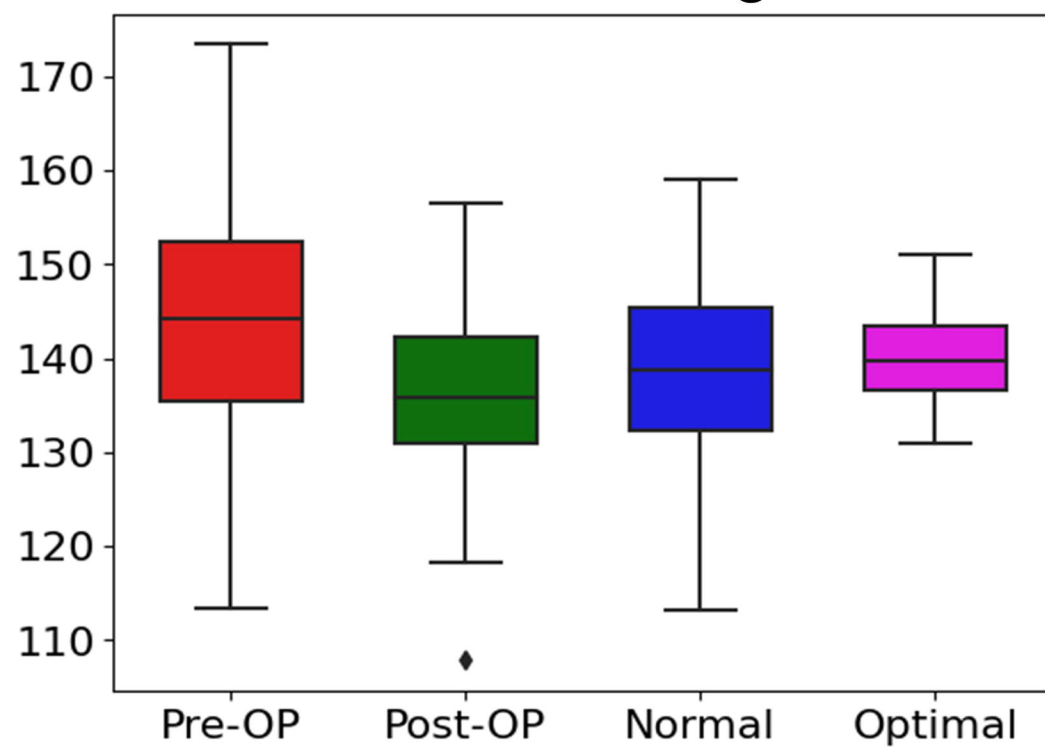
medRxiv preprint doi: <https://doi.org/10.1101/2023.12.13.23299919>; this version posted December 14, 2023. The copyright holder for this preprint (which was not certified by peer review) is the author/funder, who has granted medRxiv a license to display the preprint in perpetuity.

It is made available under a [CC-BY-NC-ND 4.0 International license](https://creativecommons.org/licenses/by-nc-nd/4.0/).

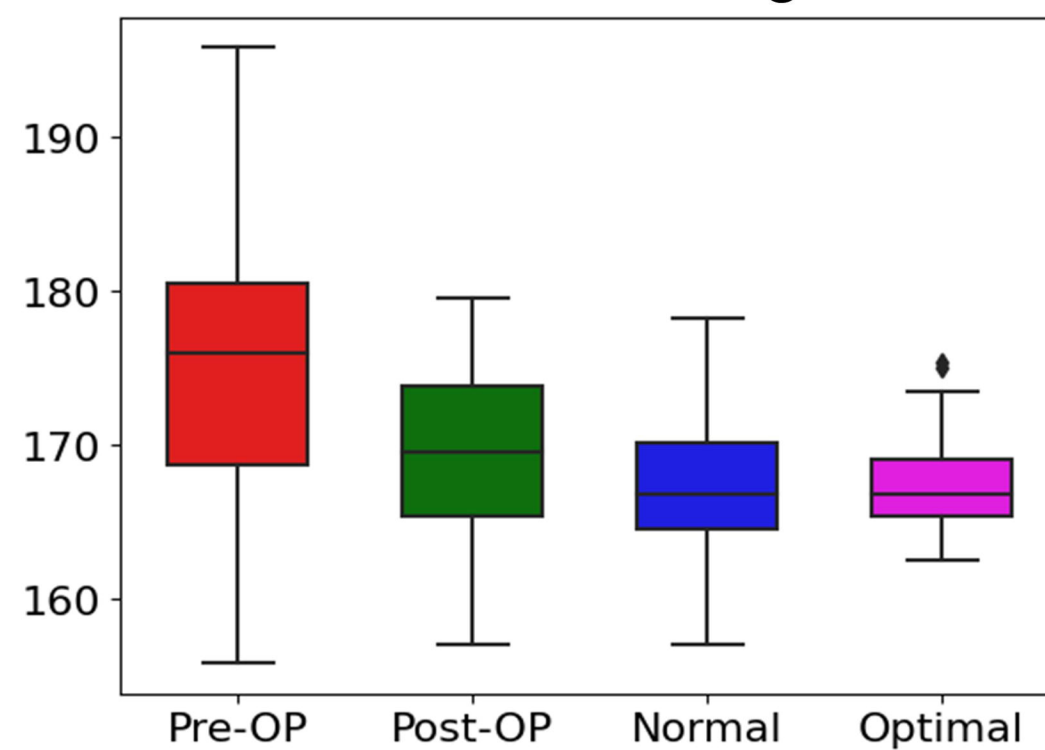
Nasolabial angle



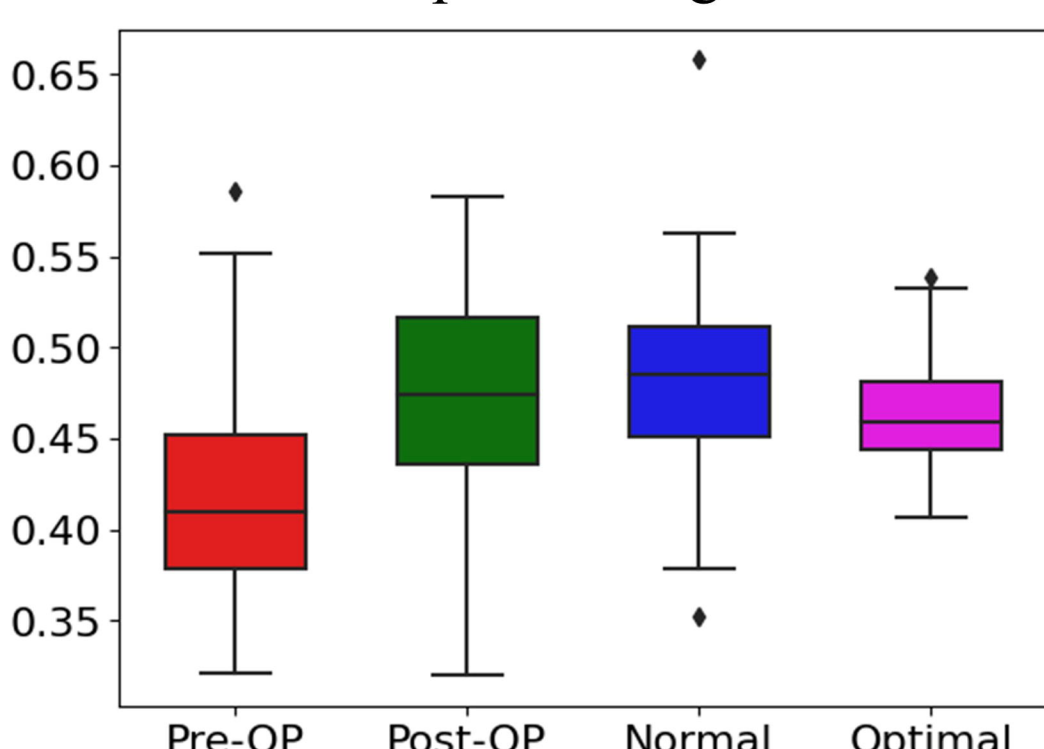
Labiomental angle



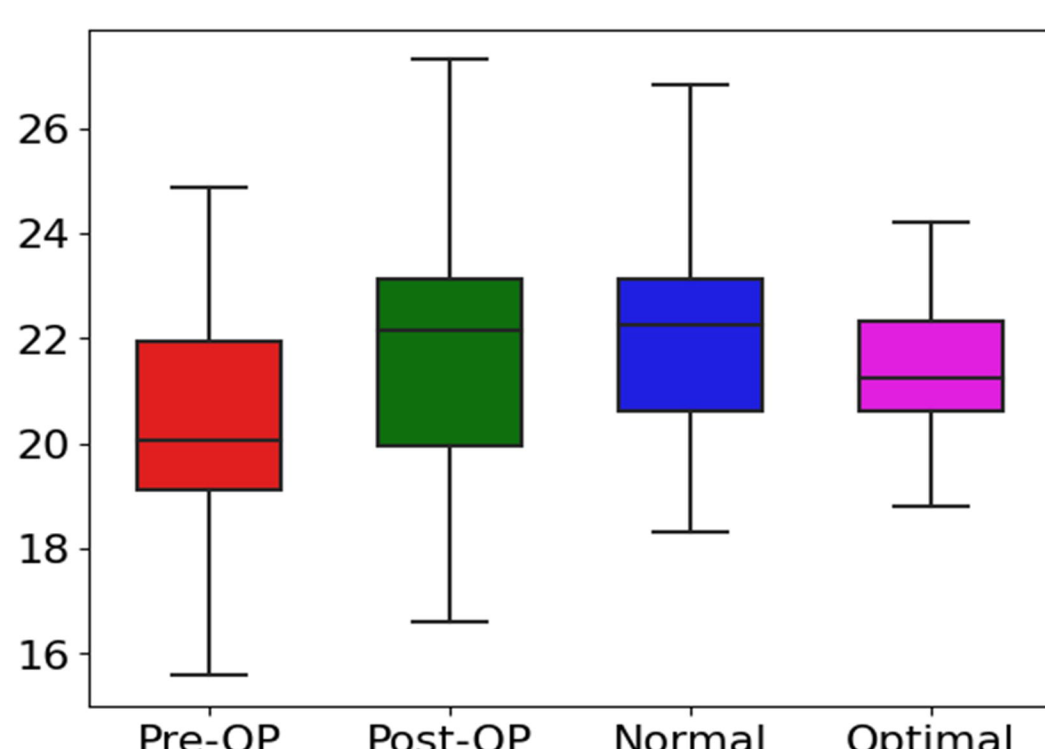
Facial contour angle



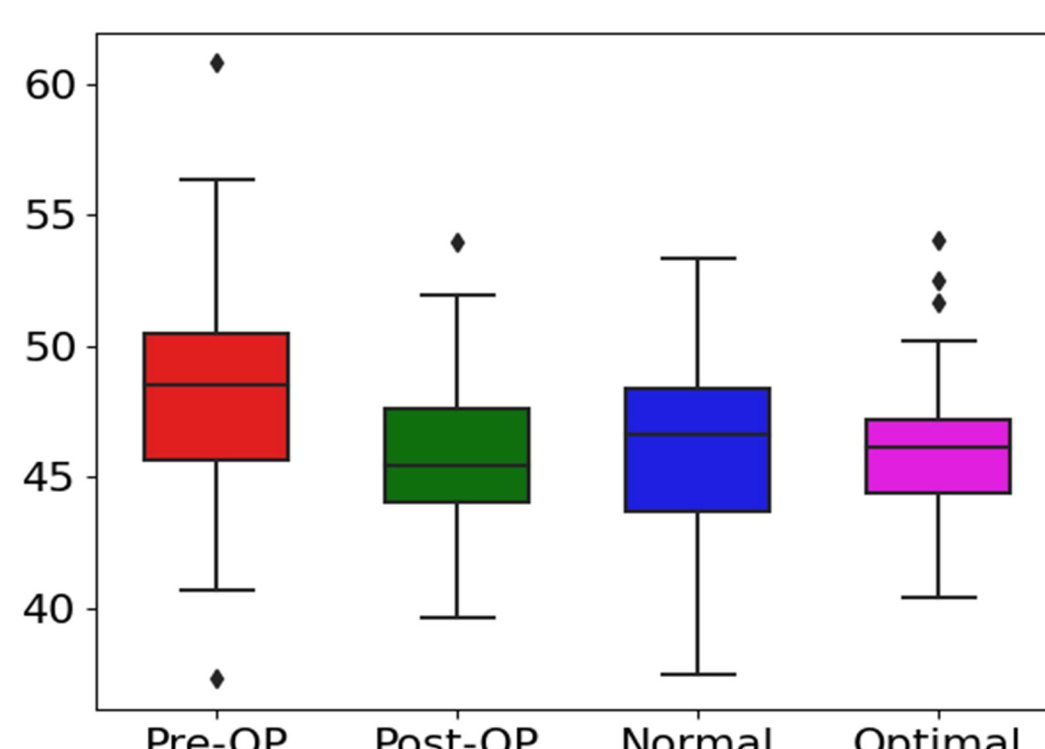
Upper lip length to lower lip-chin height ratio



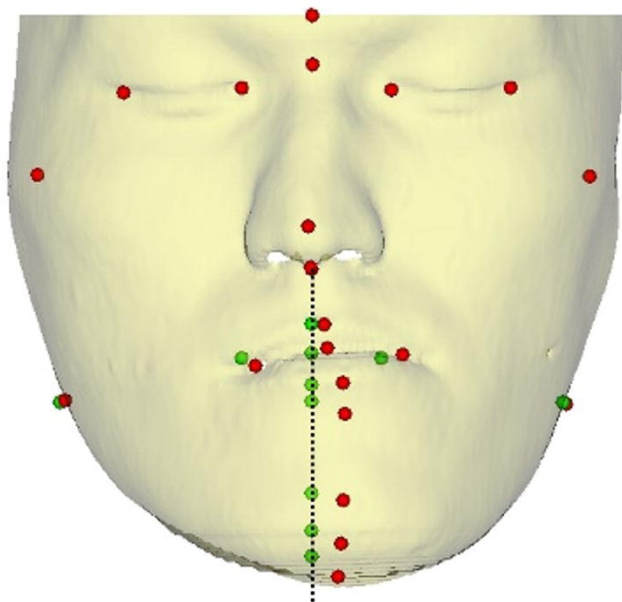
Upper lip length



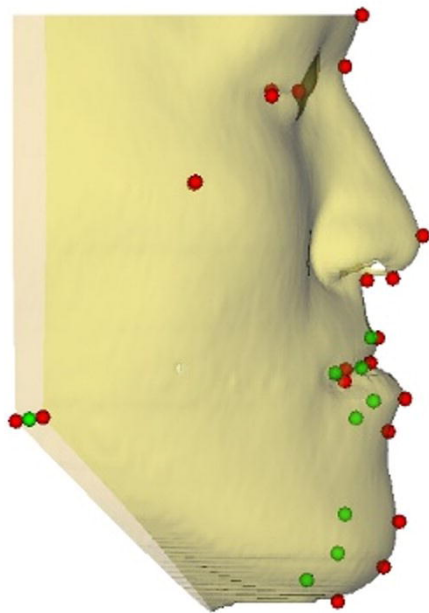
Lower lip-chin height



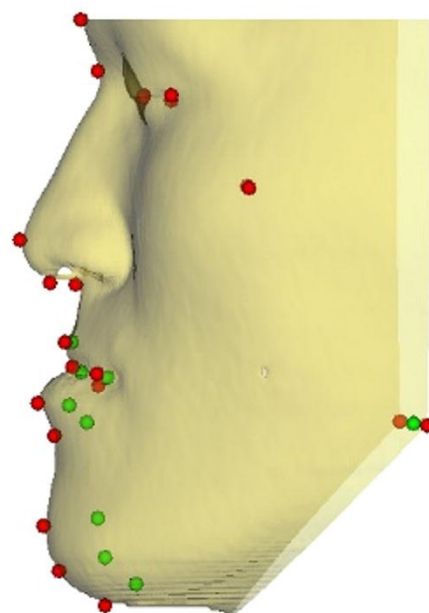
Frontal



Right



Left



● Pre-OP landmark

● Optimal landmark

⋮ Midline

## Tables

**Table 1.** Facial Landmarks

Abbreviation	Full Name
<i>Gb'</i>	Soft Tissue Glabella
<i>Prn</i>	Pronasale
<i>CM</i>	Columella
<i>Sn</i>	Subnasale
<i>Ls</i>	Labiale Superius
<i>Stm</i>	Stomium
<i>Ch-R</i>	Right Cheilion
<i>Ch-L</i>	Left Cheilion
<i>Li</i>	Labiale Inferius
<i>Sl</i>	Sublabiale
<i>Pog'</i>	Soft Tissue Pogonion
<i>Me'</i>	Soft Tissue Menton
<i>Go'-R</i>	Right Soft Tissue Gonion
<i>Go'-L</i>	Left Soft Tissue Gonion

**Table 2.** Cephalometric Measurements and Weights Used in the Optimization Approach

Category	Type	Measurement	Definition	
Facial Symmetry	Bilateral point differences	Vertical Cheilion Symmetry	The difference in the distance of <i>Ch-R</i> and <i>Ch-L</i> to the axial plane that nears the external auditory canals	
		Transverse Cheilion Symmetry	The difference in the distance of <i>Ch-R</i> and <i>Ch-L</i> to the sagittal plane	
		Anteroposterior Cheilion Symmetry	The difference in the distance of <i>Ch-R</i> and <i>Ch-L</i> to the coronal plane	
		Vertical Gonion Symmetry	The difference in the distance of <i>Go'-R</i> and <i>Go'-L</i> to the axial plane that nears the external auditory canals	
		Transverse Gonion Symmetry	The difference in the distance of <i>Go'-R</i> and <i>Go'-L</i> to the sagittal plane	
		Anteroposterior Gonion Symmetry	The difference in the distance of <i>Go'-R</i> and <i>Go'-L</i> to the coronal plane	
	<i>Midpoint Deviations from the Sagittal Plane</i>		<i>Ls</i> Midpoint Deviation	
			<i>Stm</i> Midpoint Deviation	
			<i>Li</i> Midpoint Deviation	
			<i>Pog'</i> Midpoint Deviation	
		<i>Me'</i> Midpoint Deviation		
Facial Form	Angle ( $\lambda=0.8$ )	Nasolabial Angle	$\angle (CM, Sn, Ls)$	
		Labiomental Angle	$\angle (Li, Sl, Pog')$	
		Facial Contour Angle	$\angle (Gb', Prn, Pog')$	
	Ratio ( $\lambda=0.05$ )	Upper lip length to lower lip-chin height	Distance between <i>Sn</i> and <i>Stm</i> / Distance between <i>Stm</i> and <i>Me'</i>	
		Length ( $\lambda=0.2$ )	Upper lip height	Distance between <i>Sn</i> and <i>Stm</i>
			Lower lip-chin height	Distance between <i>Stm</i> and <i>Me'</i>

$\lambda$ : Weight for optimization approach

**Table 3.** Comparison of Cephalometric Measurements between Predicted Optimal Landmarks and the Normal Subjects

Measurement metric	Measurements from the Optimized Preoperative Group		Measurements from the Normal Subject Group		Difference	
	mean $\pm$ SD	95% CI	mean $\pm$ SD	95% CI	Test	<i>p</i> -value
Vertical Cheilion Sym.	0.00 $\pm$ 0.00	0.00	0.76 $\pm$ 0.59	[0, 0.87]	MWU test	<0.001*
Transverse Cheilion Sym.	0.00 $\pm$ 0.00	0.00	0.76 $\pm$ 0.56	[0, 0.86]	MWU test	<0.001*
AP Cheilion Sym.	0.00 $\pm$ 0.00	0.00	0.98 $\pm$ 0.84	[0, 1.13]	MWU test	<0.001*
Vertical Gonion Sym.	0.00 $\pm$ 0.00	0.00	2.79 $\pm$ 1.74	[0, 3.11]	MWU test	<0.001*
Transverse Gonion Sym.	0.00 $\pm$ 0.00	0.00	1.33 $\pm$ 1.00	[0, 1.52]	MWU test	<0.001*
AP Gonion Sym.	0.00 $\pm$ 0.00	0.00	2.03 $\pm$ 1.67	[0, 2.34]	MWU test	<0.001*
<i>Ls</i> Midpoint Deviation	0.00 $\pm$ 0.00	0.00	0.38 $\pm$ 0.34	[0, 0.44]	MWU test	<0.001*
<i>Stm</i> Midpoint Deviation	0.00 $\pm$ 0.00	0.00	0.49 $\pm$ 0.38	[0, 0.56]	MWU test	<0.001*
<i>Li</i> Midpoint Deviation	0.00 $\pm$ 0.00	0.00	0.72 $\pm$ 0.47	[0, 0.80]	MWU test	<0.001*
<i>Sl</i> Midpoint Deviation	0.00 $\pm$ 0.00	0.00	0.70 $\pm$ 0.51	[0, 0.79]	MWU test	<0.001*
<i>Pog'</i> Midpoint Deviation	0.00 $\pm$ 0.00	0.00	0.84 $\pm$ 0.67	[0, 0.96]	MWU test	<0.001*
<i>Me'</i> Midpoint Deviation	0.00 $\pm$ 0.00	0.00	1.25 $\pm$ 0.97	[0, 1.43]	MWU test	<0.001*
Nasolabial angle	100.01 $\pm$ 5.54	[97.94, 102.07]	101.62 $\pm$ 9.38	[98.90, 104.34]	Welch's t	0.342
Labiomental angle	140.11 $\pm$ 5.12	[138.19, 142.02]	137.83 $\pm$ 10.02	[134.92, 140.74]	Welch's t	0.190
Facial contour angle	167.66 $\pm$ 3.34	[166.42, 168.91]	166.86 $\pm$ 4.43	[144.6, 146.8]	Ind t	0.395
Upper lip length to lower lip-chin height ratio	0.46 $\pm$ 0.04	[0.45, 0.48]	0.48 $\pm$ 0.05	[0.46, 0.50]	Welch's t	0.120
Upper lip length	21.44 $\pm$ 1.35	[20.93, 21.94]	22.07 $\pm$ 2.08	[21.47, 22.67]	Welch's t	0.106
Lower lip-chin height	46.30 $\pm$ 2.97	[45.19, 47.40]	46.17 $\pm$ 3.67	[45.11, 47.24]	Ind t	0.877

Sym: symmetry, AP: anteroposterior, SD: standard deviation, CI: confidence interval, MWU test: Mann-Whitney U test, Welch's t: Welch's t-test, Ind t: Independent t-test, \* Significant difference ( $p < 0.017$ ).

**Table 4.** Comparison of Cephalometric Measurements between Predicted Optimal Landmarks and Postoperative Patients

Measurement Metric	Measurements from the Optimized Preoperative Group		Measurements from the Postoperative Group		Difference	
	mean $\pm$ SD	95% CI	mean $\pm$ SD	95% CI	Test	<i>p</i> -value
Vertical Cheilion Sym.	0.00 $\pm$ 0.00	0.00	1.13 $\pm$ 0.94	[0, 1.34]	WSR test	<0.001*
Transverse Cheilion Sym.	0.00 $\pm$ 0.00	0.00	0.95 $\pm$ 0.93	[0, 1.17]	WSR test	<0.001*
AP Cheilion Sym.	0.00 $\pm$ 0.00	0.00	1.20 $\pm$ 0.81	[0, 1.38]	WSR test	<0.001*
Vertical Gonion Sym.	0.00 $\pm$ 0.00	0.00	5.04 $\pm$ 3.41	[0, 5.82]	WSR test	<0.001*
Transverse Gonion Sym.	0.00 $\pm$ 0.00	0.00	1.51 $\pm$ 1.17	[0, 1.78]	WSR test	<0.001*
AP Gonion Sym.	0.00 $\pm$ 0.00	0.00	3.97 $\pm$ 3.25	[0, 4.72]	WSR test	<0.001*
<i>Ls</i> Midpoint Deviation	0.00 $\pm$ 0.00	0.00	0.55 $\pm$ 0.50	[0, 0.66]	WSR test	<0.001*
<i>Stm</i> Midpoint Deviation	0.00 $\pm$ 0.00	0.00	0.75 $\pm$ 0.65	[0, 0.90]	WSR test	<0.001*
<i>Li</i> Midpoint Deviation	0.00 $\pm$ 0.00	0.00	1.12 $\pm$ 0.96	[0, 1.34]	WSR test	<0.001*
<i>SI</i> Midpoint Deviation	0.00 $\pm$ 0.00	0.00	1.46 $\pm$ 1.19	[0, 1.74]	WSR test	<0.001*
<i>Pog'</i> Midpoint Deviation	0.00 $\pm$ 0.00	0.00	2.08 $\pm$ 1.66	[0, 2.46]	WSR test	<0.001*
<i>Me'</i> Midpoint Deviation	0.00 $\pm$ 0.00	0.00	2.53 $\pm$ 1.93	[0, 2.97]	WSR test	<0.001*
Nasolabial angle	100.01 $\pm$ 5.54	[97.94, 102.07]	102.34 $\pm$ 9.29	[98.87, 105.80]	Paired t	0.024
Labiomental angle	140.11 $\pm$ 5.12	[138.19, 142.02]	135.88 $\pm$ 10.40	[132.00, 139.76]	Paired t	0.027
Facial contour angle	167.66 $\pm$ 3.34	[166.42, 168.91]	169.03 $\pm$ 6.57	[166.58, 171.49]	Paired t	0.117
Upper lip length to lower lip-chin height ratio	0.46 $\pm$ 0.04	[0.45, 0.48]	0.47 $\pm$ 0.06	[0.45, 0.50]	Paired t	0.169
Upper lip length	21.44 $\pm$ 1.35	[20.93, 21.94]	21.69 $\pm$ 2.26	[20.85, 22.53]	Paired t	0.454
Lower lip-chin height	46.30 $\pm$ 2.97	[45.19, 47.40]	45.74 $\pm$ 3.39	[44.48, 47.01]	Paired t	0.117

Sym: symmetry AP: anteroposterior, SD: standard deviation, CI: confidence interval, WSR test: Wilcoxon Signed Rank test, Paired t: Paired t-test, \* Significant difference ( $p < 0.017$ ).

**Table 5.** Comparison of Cephalometric Measurements between Postoperative Patients and Normal Subjects

Measurement metric	Measurements from the Postoperative Group		Measurements from the Normal Subject Group		Difference	
	mean $\pm$ SD	95% CI	mean $\pm$ SD	95% CI	Test	<i>p</i> -value
Vertical Cheilion Sym.	1.13 $\pm$ 0.94	[0, 1.34]	0.76 $\pm$ 0.59	[0, 0.87]	MWU test	0.130
Transverse Cheilion Sym.	0.95 $\pm$ 0.93	[0, 1.17]	0.76 $\pm$ 0.56	[0, 0.86]	Ind t	0.307
AP Cheilion Sym.	1.20 $\pm$ 0.81	[0, 1.38]	0.98 $\pm$ 0.84	[0, 1.13]	MWU test	0.174
Vertical Gonion Sym.	5.04 $\pm$ 3.41	[0, 5.82]	2.79 $\pm$ 1.74	[0, 3.11]	Welch's t	0.002*
Transverse Gonion Sym.	1.51 $\pm$ 1.17	[0, 1.78]	1.33 $\pm$ 1.00	[0, 1.52]	MWU test	0.548
AP Gonion Sym.	3.97 $\pm$ 3.25	[0, 4.72]	2.03 $\pm$ 1.67	[0, 2.34]	MWU test	0.001*
<i>Ls</i> Midpoint Deviation	0.55 $\pm$ 0.50	[0, 0.66]	0.38 $\pm$ 0.34	[0, 0.44]	MWU test	0.201
<i>Stm</i> Midpoint Deviation	0.75 $\pm$ 0.65	[0, 0.90]	0.49 $\pm$ 0.38	[0, 0.56]	MWU test	0.108
<i>Li</i> Midpoint Deviation	1.12 $\pm$ 0.96	[0, 1.34]	0.72 $\pm$ 0.47	[0, 0.80]	Welch's t	0.040
<i>Sl</i> Midpoint Deviation	1.46 $\pm$ 1.19	[0, 1.74]	0.70 $\pm$ 0.51	[0, 0.79]	MWU test	0.004*
<i>Pog'</i> Midpoint Deviation	2.08 $\pm$ 1.66	[0, 2.46]	0.84 $\pm$ 0.67	[0, 0.96]	MWU test	<0.001*
<i>Me'</i> Midpoint Deviation	2.53 $\pm$ 1.93	[0, 2.97]	1.25 $\pm$ 0.97	[0, 1.43]	MWU test	<0.001*
Nasolabial angle	102.34 $\pm$ 9.29	[98.87, 105.80]	101.62 $\pm$ 9.38	[98.90, 104.34]	Ind t	0.743
Labiomental angle	135.88 $\pm$ 10.40	[132.00, 139.76]	137.83 $\pm$ 10.02	[134.92, 140.74]	Ind t	0.412
Facial contour angle	169.03 $\pm$ 6.57	[166.58, 171.49]	166.86 $\pm$ 4.43	[144.6, 146.8]	Welch's t	0.116
Upper lip length to lower lip-chin height ratio	0.47 $\pm$ 0.06	[0.45, 0.50]	0.48 $\pm$ 0.05	[0.46, 0.50]	Ind t	0.779
Upper lip length	21.69 $\pm$ 2.26	[20.85, 22.53]	22.07 $\pm$ 2.08	[21.47, 22.67]	Ind t	0.449
Lower lip-chin height	45.74 $\pm$ 3.39	[44.48, 47.01]	46.17 $\pm$ 3.67	[45.11, 47.24]	Ind t	0.607

Sym: symmetry, AP : anteroposterior, SD: standard deviation, CI:confidence interval, MWU test: Mann-Whitney U test, Welch's t: Welch's t-test, Ind t: Independent t-test, \* Significant difference ( $p < 0.017$ ).